PHYSICAL REVIEW B **80**, 121401(R) (2009)

Structure of the fivefold surface of the Ag-In-Yb icosahedral quasicrystal

H. R. Sharma,[1,*] M. Shimoda,[2] K. Sagisaka,[2] H. Takakura,[3] J. A. Smerdon,[1] P. J. Nugent,[1] R. McGrath,[1] D. Fujita,[2] S. Ohhashi,[4] and A. P. Tsai[2,4]

[1]*Surface Science Research Centre and Department of Physics, The University of Liverpool, Liverpool L69 3BX, United Kingdom*

[2]*National Institute for Materials Science, 1-2-1 Sengen, Tsukuba, Ibaraki 305-0047, Japan*

[3]*Division of Applied Physics, Graduate School of Engineering, Hokkaido University, Sapporo 060-8628, Japan*

[4]*Institute of Multidisciplinary Research for Advanced Materials, Tohoku University, Sendai 980-8577, Japan*

(Received 10 June 2009; published 3 September 2009)

The surface structural study of an icosahedral (*i*) quasicrystal of the Cd-Yb family is presented. Comparison of bias-dependent scanning tunneling microscopy data from the fivefold surface of *i*-Ag-In-Yb with the refined bulk model of isostructural *i*-Cd-Yb indicates that surfaces are formed at bulk planes intersecting the center of the rhombic triacontahedral clusters, the building blocks of the Cd-Yb family quasicrystals. These observations open up the possibility of the use of this material as a template for epitaxial structures.

DOI: 10.1103/PhysRevB.80.121401 PACS number(s): 61.44.Br, 68.35.B−, 68.37.Ef

Icosahedral quasicrystals are three-dimensional solids which differ from conventional crystals in that they possess long-range order without periodicity. Studies of their surfaces have been restricted to Al-based systems whose structure can be described in terms of pseudo-Mackay and Bergman clusters.[1] Here, we present the surface structural studies of an icosahedral (*i*) quasicrystal of the Cd-Yb family, whose basic building block is the rhombic triacontahedral (RTH) cluster.[2] We compare scanning tunneling microscopy (STM) measurements of the fivefold *i*-Ag-In-Yb surface with the bulk structure model of isostructural *i*-Cd-Yb.

The unusual physical properties of icosahedral quasicrystals[3] have led to a quest for detailed structural information on these aperiodic materials. Although significant progress has been made in applying diffraction techniques to trimetallic icosahedral quasicrystals, particularly in the case of *i*-Al-Pd-Mn,[4] a full structural determination has proved elusive. The discovery of the binary *i*-$Cd_{5.7}Yb$ quasicrystal in 2000 (Ref. 2) was immediately recognized as a major advance.[5] The chemical order and structural perfection of *i*-$Cd_{5.7}Yb$, together with the existence of the 1/1 cubic approximant crystal $YbCd_6$ and the 2/1 cubic approximant $YbCd_{5.8}$ led to full structural solution of an icosahedral quasicrystal.[6] The structure can be described as an aperiodic arrangement of RTH clusters. Atoms belonging to the RTH units constitute 93.8% of the total.[6] Cd and Yb atoms in the interstices (glue atoms) can be precisely specified using the acute rhombohedron (AR) and obtuse rhombohedron (OR) units in the proposed model.[6]

A consensus has developed that surfaces of the Al-Mn class of quasicrystals prepared under suitable conditions correspond to terminations of the bulk structure with minimal structural relaxation.[7–10] This in turn has led to their application as templates for growth studies and hence to the discovery of several phenomena which have extended our understanding of epitaxy. These include quasiperiodically modulated multilayer Cu structures,[11,12] pseudomorphic monolayers of Pb,[13,14] Bi,[15,16] and Sb (Ref. 17) and island growth influenced by quantum size effects.[18]

The surfaces of the binary *i*-$Cd_{5.7}Yb$ would undoubtedly provide possibilities for the discovery of further new phenomena in epitaxial growth. Truncations of the rather different structure of the RTH cluster would give rise to geometrical and chemical surface patterns. A major difficulty exists in realizing this objective: the *i*-$Cd_{5.7}Yb$ quasicrystal is not suitable for surface preparation in ultrahigh-vacuum (UHV) conditions because the high vapor pressure of Cd leads to evaporation upon heat treatment. A resolution of this dilemma has been provided by the discovery of *i*-Ag-In-Yb quasicrystal[19,20] which is isostructural to *i*-$Cd_{5.7}Yb$. Replacement of Cd by equal percentages of Ag and In was found to maintain the valence electron to atom ratio of 2.0,[19,20] which is necessary condition for the formation of this type of quasicrystals. As Ag and In are both stable in UHV, surface studies of this icosahedral quasicrystal are therefore feasible.

The Bridgman method was employed to grow the single grain sample with resulting composition of *i*-$Ag_{42}In_{42}Yb_{16}$.[19,20] The sample was then cut perpendicular to the fivefold axis determined by Laue backscattering and polished using diamond paste down to 0.25 μm. Subsequently, the surface was cleaned using repeated cycles of Ar^+ sputtering (1–3 keV, 30–60 min) and annealing (at 715 K for 2–3 h) under UHV (base pressure 2×10^{-10} mbar). After sputtering the surface shows a depletion of In and Yb. Annealing recovers the bulk composition at the surface.[21] STM measurements were performed on the annealed surface using an Omicron STM operating at room temperature as well as a Unisoku low-temperature STM operating at 78 K. No difference was observed in STM contrast at room temperature and low temperature.

After annealing, the surface displays terraces and steps of different heights as shown in Figs. 1(a) and 1(b). Low-energy electron diffraction (LEED) patterns from the surface show discrete spots distributed with fivefold symmetry and with successive spots located at τ-scaling distances, $\tau=1.618\ldots$ being the golden mean: a characteristic number related to pentagonal symmetry [Fig. 1(c)]. This is indicative of quasicrystalline long-range order of the surface.

The steps are of different heights. In order to determine the height distribution we selected about 400 steps from STM images taken from different parts of the surface and obtained in different cleaning cycles. Average heights of individual steps were calculated from the height histogram of the measured z values [Fig. 1(d)]. The step heights are close

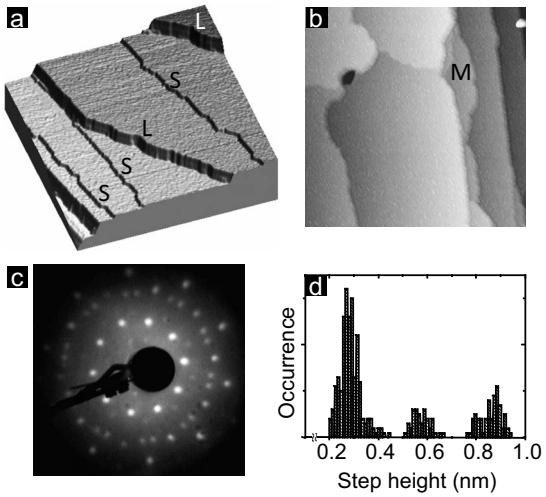

FIG. 1. [(a) and (b)] Large scale STM images of the fivefold i-$Ag_{42}In_{42}Yb_{16}$ surface taken at room temperature (a) 3D view, area $(A)=250$ nm$\times 250$ nm, bias voltage $(V_B)=-0.8$ V, tunneling current $(I_T)=0.40$ nA and (b) $A=300$ nm$\times 300$ nm, $V_B=+1.1$ V, $I_T=0.35$ nA). Steps of different heights are marked [$S=0.28(\pm 0.04)$ nm, $M=0.58(\pm 0.03)$ nm, and $L\sim M+S=0.85(\pm 0.05)$ nm]. (c) LEED pattern from the same surface (electron energy: 23 eV). (d) The distribution of step heights determined from measurements of 400 steps.

to three values: $S=0.28(\pm 0.04)$ nm, $M=0.58(\pm 0.03)$ nm ~ 2 S, and $L\sim M+S=0.85(\pm 0.05)$ nm. Occasionally, these steps bunch together to form higher steps, which are not considered in Fig. 1(d). The L and S steps frequently show a local configuration of *LSLSS* as seen in Fig. 1(a). The occurrence of the S, M, and L steps is, respectively, 66%, 12%, and 22%. The low occurrence of the M steps as well as the fact that the terraces with these steps are very narrow [see Fig. 1(b)] suggests that surface termination arising from the presence of the M steps is less preferred.

STM images of the terraces are found to be dependent on the applied bias voltage (V_B). Figures 2(a)–2(d) shows STM images taken from the same portion of a terrace with the same tip at positive and negative sample bias. The stability of the tip was confirmed by reproducing the original images after the measurements. At $V_B<0$ electrons tunnel from occupied sample states to unoccupied tip states and thus the occupied states of the sample are probed, while at $V_B>0$ the unoccupied states of the sample are detected.

The images at $V_B<0$ are characterized by large protrusions, which are locally arranged in pentagons [circled in Figs. 2(a) and 2(c)]. The pentagons have an edge length of $2.40(\pm 0.15)$ nm and have two different orientations rotated by 36° from each other. The diameter of the protrusions estimated from the full width at half maxima of height profiles is $1.30(\pm 0.04)$ nm.

For $V_B>0$, the protrusions do not appear: instead, rings are observed at the vertices of the pentagons. The diameter of the rings is $1.80(\pm 0.05)$ nm. The Fourier transforms of the STM images at both positive and negative bias show a tenfold pattern with maxima located at τ-scaling distances (not shown) confirming quasicrystalline long-range order in agreement with the LEED results described above.

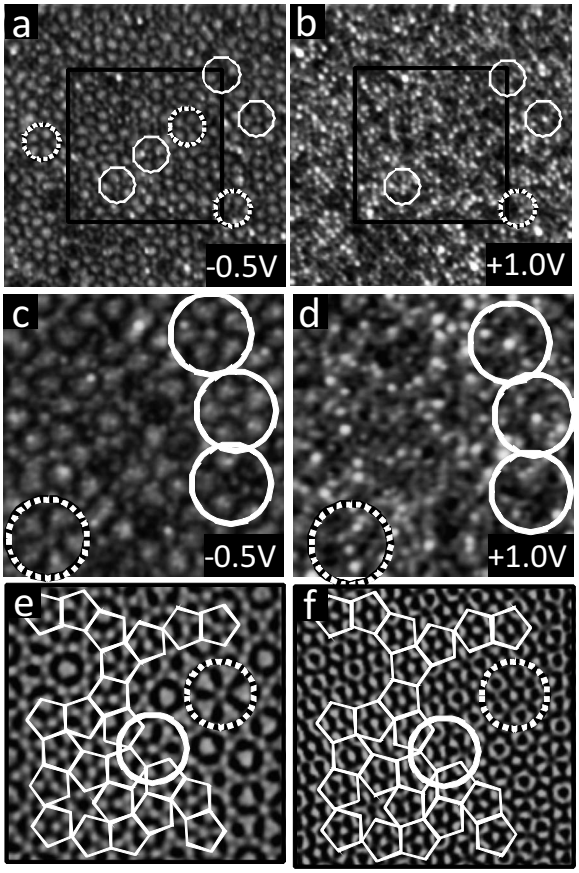

FIG. 2. High-resolution STM images of the fivefold i-$Ag_{42}In_{42}Yb_{16}$ surface. [(a) and (c)] Images taken at negative bias. [(b) and (d)] Images taken at positive bias [(a) and (b): 49 nm $\times 49$ nm; (c) and (d): 23 nm$\times 23$ nm; $I_T=1.3$ nA, tunneling temperature: 78 K]. The full and dotted circles mark pentagonal features of two different orientations. [(e) and (f)] Area marked by a frame in (a) and (b) after Fourier transform pass filtering and with a pentagonal tiling overlaid.

After Fourier transform pass filtering of images in Figs. 2(a) and 2(b), the protrusions and rings appear enhanced [Figs. 2(e) and 2(f)]. The STM image at $V_B<0$ can be overlaid by pentagonal tiles whose vertices are located at the center of the protrusions [Fig. 2(e)]. The edge length of the tiles is $2.40(\pm 0.15)$ nm. The same tiling can be superimposed on the image at $V_B>0$, where the vertices of the tiling now fall in the center of rings, rather than protrusions [Fig. 2(f)].

We next compare the experimental observations described above to the model of the bulk structure of i-Cd-Yb. The RTH units consist of five successive atomic shells.[6] The fifth (outermost), fourth, and second shells are, respectively, a rhombic triacontahedron (diameter 1.56 nm, 92 Cd atoms), an icosidodecahedron (diameter 1.3 nm, 30 Cd atoms), and a dodecahedron (diameter 0.92 nm, 20 Cd atoms). The innermost shell is composed of four Cd atoms which form a tetrahedron. The third shell, which is an icosahedron (diameter 1.12 nm), is occupied by 12 Yb atoms. Figure 3 shows the three-dimensional atomic structure in the model normal to the fivefold axis (z axis)[6] after structural refinement using x-ray diffraction data. The variation in atomic density along

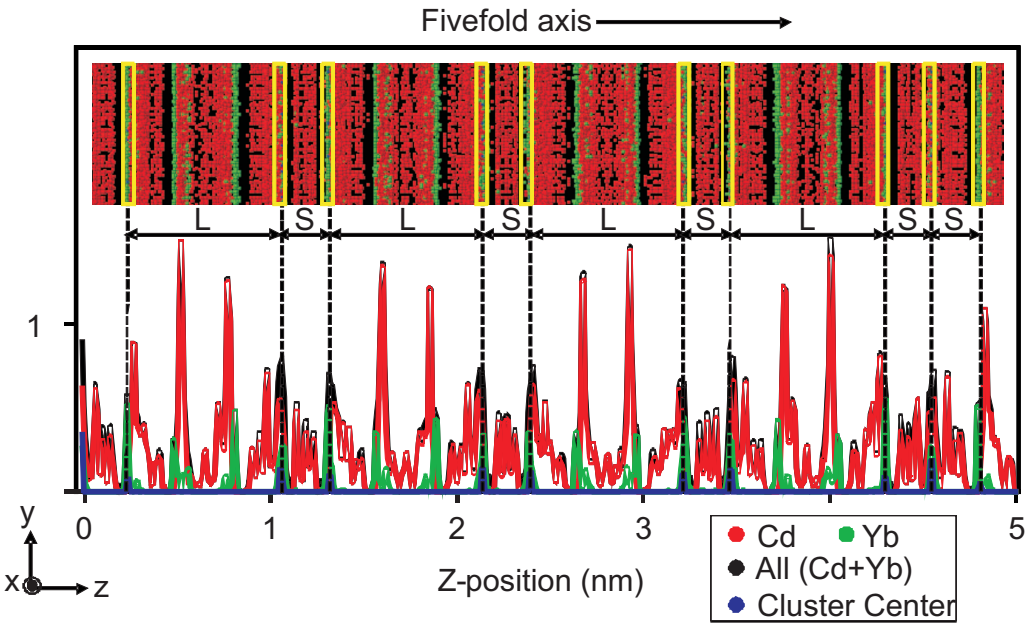

FIG. 3. (Color) Top: atomic structure of *i*-Cd-Yb projected normal to the fivefold axis (red: Cd and green: Yb, *y* axis is compressed). Atomic positions were obtained after structural refinement using x-ray diffraction data. The refinement results in shifts of a group of atoms from their idealized positions and atomically flat layers of the ideal structure are modified into puckered layers. High-density regions intersecting the cluster centers are marked by yellow rectangles. Bottom: variation in atomic density in layers perpendicular to the fivefold axis (red: Cd, green: Yb, black: total, blue: cluster centers, density of which is not in scale). For the plot, we considered a step of $\Delta z = 0.05$ nm. The maximum projected atomic density in this region is comparable to that of the closed-packed Yb surface. The position of the cluster centers is marked by dotted lines. The high-density peaks are separated by 0.27 nm(± 0.01) nm.

the fivefold axis calculated from a slab of 10 nm$\times$10 nm $\times$5 nm is also given in Fig. 3. The high-density regions are clearly separated by gaps (lower density regions), which is consistent with the electron density analysis of the same system reported by de Boissieu *at el*.[22] The Yb layers are always associated with high-density regions and they are separated by 0.25 nm. The majority of these Yb layers intersect the RTH cluster centers.

The experimental evidence indicates that the terraces observed in STM are formed at the high-density regions which intersect the cluster centers. The separation of the selected high-density layers in the model (marked in Fig. 3 by yellow rectangles) is close to the observed step heights $S(=0.28 \pm 0.04$ nm) and $L(=0.85 \pm 0.05$ nm). The frequency of occurrence of the *S* steps estimated from a slab of the model of 10 nm$\times$10 nm$\times$10 nm is about 60%, which is in reasonable agreement with the value of 66% deduced from the measurements. The selected terminations do not produce *M* steps, which is consistent with the low preference of the *M* steps observed by STM. The sequence of *LSLSS* observed by STM can be identified in the model terminations shown in Fig. 3. Finally and crucially, surface termination at every high-density layer (not just those corresponding to cluster centers) would yield only *S* steps. This would not agree with the observation of *L* steps in STM.

The formation of the terraces at selected regions is further evidenced by comparing the atomic structure of the cluster-center terminations in the model with the bias-dependent STM images of the terraces. A tiling of 2.53 nm edge length can be superimposed in these terminations [Fig. 4(a)] which is consistent with the 2.40(± 0.15) nm pentagonal tiling of the STM images. Almost all of the vertices of the tiling superimposed on the model coincide with the cluster centers. The vertices are decorated by concentric rings of atoms. The first ring from the center (red) corresponds to the cross-section of the Cd icosidodecahedron (the fourth shell of the RTH cluster) and has diameter 1.30 nm. This ring contains

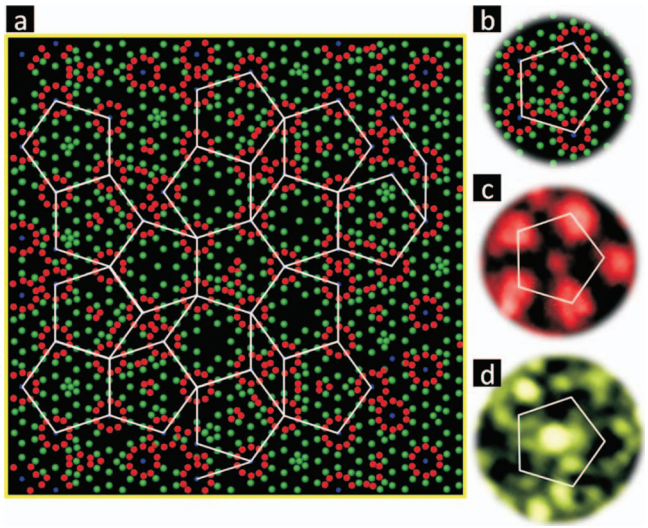

FIG. 4. (Color) (a) The projected in-plane structure of the regions marked by a yellow rectangles in Fig. 3 (area: 10 nm $\times$10 nm, $\Delta z = 0.05$ nm). (b) Pentagonal motifs from the in-plane structure with edge length of 2.53 nm and from STM images at (c) negative and (d) positive biases with edge length of 2.40(± 0.15) nm.

both Ag and In; the exact distribution of Ag and In atoms in the ring is not known. The diameter of the protrusions observed in STM (1.30 ± 0.04 nm) matches that of the Ag/In ring in the model. This indicates that the tunneling current at $V_B < 0$ is enhanced at the Ag or In sites and suppressed at the Yb sites. The lack of atomic resolution in the protrusions may be due to electronic coupling of the Ag and In atoms.

The second ring from the center of the RHT cluster center (green) has a diameter of 1.94 nm and contains Yb atoms. The ring is incomplete at some of the vertices. These Yb atoms belong to different RTH units or linkages between the RTH units. The diameter of the ring is close to the diameter of the ring observed in STM at $V_B > 0 (1.80 \pm 0.05$ nm). This indicates that the tunneling current at $V_B > 0$ is enhanced at the Yb sites. This is consistent with *ab initio* studies of *i*-Cd-Yb which show that the unoccupied states just above the Fermi level are dominated by Yb-5*d* levels.[23]

In summary, based on STM measurements from the fivefold *i*-Ag-In-Yb surface and the bulk model structure of *i*-Cd-Yb, we find that the surface forms preferentially at bulk positions which are dense and intersect the cluster centers. The truncated RTH clusters are arranged in a dense quasiperiodic array which is chemically well defined. These findings open up the possibility of the use of these surfaces as templates for epitaxial meta structures.

This work was supported by Engineering and Physical Sciences Research Council (Grants No. EP/D071828/1 and No. EP/DO5253X/1). We would like to thank V. Fournée at CNRS Nancy for a critical reading of this Rapid Communication and valuable suggestions.

*Corresponding author; h.r.sharma@liv.ac.uk

[1] D. Gratias, F. Puyraimond, M. Quiquandon, and A. Katz, Phys. Rev. B **63**, 024202 (2000).
[2] A. P. Tsai, J. Q. Guo, E. Abe, H. Takakura, and T. J. Sato, Nature (London) **408**, 537 (2000).
[3] H.-R. Trebin, *Quasicrystals: Structure and Physical Properties* (Wiley-VCH, Berlin, 2003).
[4] A. Yamamoto, H. Takakura, and A. P. Tsai, Phys. Rev. B **68**, 094201 (2003).
[5] P. A. Thiel and J. M. Dubois, Nature (London) **406**, 570 (2000).
[6] H. Takakura, C. P. Gomez, A. Yamamoto, M. D. Boissieu, and A. P. Tsai, Nature Mater. **6**, 58 (2007).
[7] H. R. Sharma, M. Shimoda, and A. P. Tsai, Adv. Phys. **56**, 403 (2007).
[8] Z. Papadopolos, G. Kasner, J. Ledieu, E. J. Cox, N. V. Richardson, Q. Chen, R. D. Diehl, T. A. Lograsso, A. R. Ross, and R. McGrath, Phys. Rev. B **66**, 184207 (2002).
[9] M. Gierer, M. A. Van Hove, A. I. Goldman, Z. Shen, S.-L. Chang, C. J. Jenks, C.-M. Zhang, and P. A. Thiel, Phys. Rev. Lett. **78**, 467 (1997).
[10] L. Barbier, D. Le Floch, Y. Calvayrac, and D. Gratias, Phys. Rev. Lett. **88**, 085506 (2002).
[11] J. Ledieu, J. T. Hoeft, D. E. Reid, J. A. Smerdon, R. D. Diehl, T. A. Lograsso, A. R. Ross, and R. McGrath, Phys. Rev. Lett. **92**, 135507 (2004).
[12] J. Ledieu, J. T. Hoeft, D. E. Reid, J. A. Smerdon, R. D. Diehl, N. Ferralis, T. A. Lograsso, A. R. Ross, and R. McGrath, Phys. Rev. B **72**, 035420 (2005).
[13] J. Ledieu, L. Leung, L. H. Wearing, R. McGrath, T. A. Lograsso, D. Wu, and V. Fournée, Phys. Rev. B **77**, 073409 (2008).
[14] J. A. Smerdon, L. Leung, J. K. Parle, C. J. Jenks, R. McGrath, V. Fournée, and J. Ledieu, Surf. Sci. **602**, 2496 (2008).
[15] K. J. Franke, H. R. Sharma, W. Theis, P. Gille, P. Ebert, and K. H. Rieder, Phys. Rev. Lett. **89**, 156104 (2002).
[16] J. A. Smerdon, J. K. Parle, L. H. Wearing, T. A. Lograsso, A. R. Ross, and R. McGrath, Phys. Rev. B **78**, 075407 (2008).
[17] H. R. Sharma, M. Shimoda, V. Fournée, A. R. Ross, T. A. Lograsso, and A. P. Tsai, Phys. Rev. B **71**, 224201 (2005).
[18] V. Fournée, H. R. Sharma, M. Shimoda, A. P. Tsai, B. Unal, A. R. Ross, T. A. Lograsso, and P. A. Thiel, Phys. Rev. Lett. **95**, 155504 (2005).
[19] J. Q. Guo and A. P. Tsai, Philos. Mag. Lett. **82**, 349 (2002).
[20] S. Ohhashi, J. Hasegawa, S. Takeuchi, and A. P. Tsai, Philos. Mag. **87**, 3089 (2007).
[21] H. R. Sharma, M. Shimoda, S. Ohhashi, and A. P. Tsai, Philos. Mag. **87**, 2989 (2007).
[22] M. de Boissieu, H. Takakura, C. P. Gomez, A. Yamamoto, and A. P. Tsai, Philos. Mag. **87**, 2613 (2007).
[23] Y. Ishii and T. Fujiwara, Phys. Rev. Lett. **87**, 206408 (2001).